

Photophysics and photochemistry of *p*-nitroaniline as photoinitiator

A. Costela ^a, I. García-Moreno ^{a,*}, J. Dabrio ^b, R. Sastre ^b

^a Instituto de Química-Física "Rocasolano", C.S.I.C., Serrano 119, Madrid 28006, Spain

^b Instituto de Ciencia y Tecnología de Polímeros, C.S.I.C., Juan de la Cierva 3, Madrid 28006, Spain

Received 30 January 1997

Abstract

Steady-state (313 and 365 nm) and laser (308 and 337 nm) photolysis have been employed to carry out a structure–reactivity investigation on *p*-nitroaniline as photoinitiator of polymerization. Detailed studies on the spectroscopy of the molecule were accomplished. Quantum yields of *p*-nitroaniline photoreduction induced by a tertiary amine, 2-(*N,N*-diethylamino)ethanol have been determined. The dependence of the photoreduction behaviour on several factors, such as photoinitiator concentration, proportion of the aliphatic amine added to *p*-nitroaniline as reducing agent, nature of the coinitiator, irradiation energy, and wavelength has been studied. The analysis by gas chromatography–mass spectroscopy technique of the photolysed solutions allowed 1,4-benzenediamine to be identified as the main photoreduction product. A mechanism for the *p*-nitroaniline photoreduction induced by the aliphatic amine is suggested. © 1997 Elsevier Science S.A.

Keywords: Photoinitiator; Nitroaniline; Laser photochemistry

1. Introduction

There is a great interest in developing photoinitiators for specific applications, which requires the ability to predict the relationship between molecular structure and properties. Nitronaphthylamine derivatives have been proposed as photoinitiators because their triplet states, formed at high yield under UV irradiation, abstract efficiently hydrogen atoms generating free radicals [1,2]. However, the high prices of these compounds are an important limitation in their commercial use as photoinitiators of polymerization processes in coatings, lacquers or ink formulations. The aim of improving existing formulations and developing better quality and more efficient bimolecular photoinitiators led us to explore the potential of *p*-nitroaniline (*p*NA) as a photoinitiator. This compound, which keeps the nitro-aromatic structure, is economically favourable and can be synthesized with high yields [3].

*p*NA is a polar molecule that has been of interest to photochemists owing to the possibility of intramolecular charge transfer effects; i.e. the molecule is bifunctional, possessing an electron donor and an acceptor group [4]. However, the studies on the *p*NA photochemistry have been by no means exhaustive. This nitrobenzene derivative has been found to undergo intermolecular hydrogen abstraction although it has

shown certain stability towards both photoreduction and photosubstitution [5].

*p*NA is known to present only phosphorescence, which indicates a high intersystem crossing [6], but the short lifetime of its triplet state at room temperature [4,7] has made difficult the study of its properties. A proper characterization of the triplet state would require the use of laser-flash photolysis technique.

Laser irradiation often leads to dramatic differences when compared with conventional lamp irradiation at a similar wavelength [8], because of the presence of laser-induced processes due to the relatively high concentration of transient intermediates generated within the duration of the laser pulse. In cases where the transient species have significant absorption at the laser excitation wavelength, they may compete with ground-state precursors for the absorption of the incident photons. Nevertheless, a quantitative analysis of photochemical events resulting from sequential two-photon processes within a single laser pulse, although inherently complex, has allowed to study the behaviour of excited reaction intermediates [9].

A detailed understanding of the mechanism of any photochemical reaction would provide the means to control the undesired processes that may take place. To this end, it is essential to collect extensive data on the rate constants and information on transients involved in the reaction.

With this aim in mind, and in order to determine the quality and efficiency of *p*NA as photoinitiator, in this paper we

* Corresponding author.

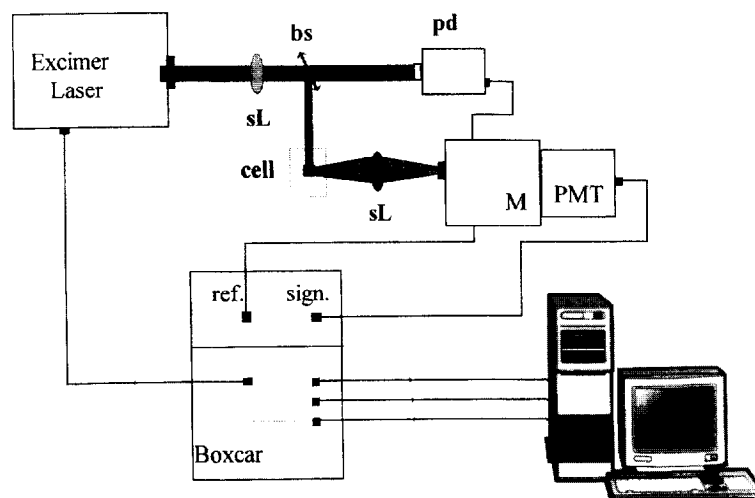


Fig. 1. Schematic diagram of experimental arrangement for laser pulsed photolysis of *p*-nitroaniline. sL = spherical lens, bs = beam splitter, pd = photodiode, M = monochromator, PMT = photomultiplier.

analyse in detail the photophysical and photochemical behaviour of *p*NA molecule under both steady-state and laser irradiation conditions. The spectral and temporal characteristics of the lowest triplet-state of *p*NA are studied by time-resolved spectroscopy. The photoreduction quantum yields of *p*NA induced either by a tertiary amine, 2-(*N,N*-diethylamino)ethanol (DEELA), or by 2-propanol (IPA), acting as coinitiators, have been determined. The dependence of the photoreduction efficiency on the nature of the reducing agent allows to establish the relative contribution of the two reaction pathways (electron–proton transfer and hydrogen atom transfer) which may be competitively involved in the *p*NA photoreduction. The detection and identification of transient species by laser induced fluorescence (LIF) and of products photochemically stable by conventional analytic techniques allows to propose a mechanism for the *p*NA photoreduction.

2. Experimental system

2.1. Steady-state photolysis

Irradiation wavelengths, 313 nm and 365 nm, were selected from a Philips high pressure mercury lamp (Hg-CS 500/2) with a Kratos model GM 252 monochromator. The irradiation system and the experimental procedure have been previously described [10]. Sample solutions were prepared by standard methods. The solutions were deoxygenated (up to less than 5 ppm) by bubbling nitrogen (L-48) or argon (L-55) gas through them for 30 min. Some experiments were carried out under aerobic conditions in order to determine the influence of oxygen on the photoreduction process. The absorbed light intensity at the irradiation wavelength was measured using an International Light digital radiometer (model II700). An Aberchrome 540 actinometer [11] was used to relate the digital display of the radiometer to an absolute value for the number of quanta incident per unit of time. The photolysis of the sample was monitored by measuring

the absorbance decrease in the maximum at the longest wavelength in the UV absorption curve.

2.2. Nanosecond laser pulsed photolysis

The experimental arrangement is indicated schematically in Fig. 1. Laser photolysis of *p*NA was carried out using a commercial XeCl excimer laser (MPB-150) supplying up to 120 mJ energy in ≈ 30 ns FWHM pulses at 308 nm. A quartz beam splitter selected $\approx 10\%$ of the laser output to be directed towards the 1 cm silica cell containing the solutions. A 1 m focal length Spectrosil B spherical lens focused mildly the photolysis light onto the cell, and a 2 mm iris diaphragm placed before the cell selected the central part of the rectangular laser beam assuring spatial uniformity of the light illuminating the sample. The total energy of the pulse impinging the cell was estimated to be ≈ 3 mJ. A fraction of the laser light passing through the beam splitter was collected by an optical fibre and directed towards a photodiode (RS-BPX-65). The signal from this photodiode was used for monitoring the photolysis laser power and for triggering the detection system.

A home-made N₂ laser supplying up to 3 mJ energy in ≈ 10 ns FWHM pulses at 337 nm was used as a second excitation source. In this case, a flat aluminium mirror ($\Phi = 5$ cm and $\lambda/20$) directed the pump laser beam towards the photolysis cell, and a 0.5 m focal length spectrosil B spherical lens was used to focus the excitation radiation into the sample cell. The total energy of the photolysis pulse in the input face of the cell was estimated to be ≈ 1 mJ. A fraction of the excitation light scattered from the lens was monitored by a fast photodiode (EG, G, SGD-100) and used for triggering purposes.

The luminescence emitted from the irradiated sample, monitored at right angles to the path beam, was imaged, after passing through a cut-off filter to eliminate scattered light from the pump laser, onto the input slit of a monochromator (MacPherson-2035, 0.35 m) and detected with a photomul-

tiplier (EMI 9816-QB). The width of the monochromator's slits was set at 250 μm , providing a spectral resolution of ≈ 0.5 nm. The signal from the photomultiplier was either sent to the 50 Ω input of a 40 MHz digital oscilloscope (Tektronix 2430A; rise time = 10 ns and vertical resolution = 8 bits) for real time measurements or, for spectra recording, fed to a box-car (Stanford SR-250) to be integrated before being digitized by a SR-245 A/D converter. A personal computer via a ComputerBoard DASH-8 interface was used to record the signal as well as to control and synchronize the whole experiment. Complementary details of the operation of this system have been described elsewhere [12,13].

Sample solutions for the laser experiments were prepared by standard methods. Degassing of the samples was accomplished by the "freeze and thaw method" pumping down to pressures below 10^{-4} Torr. The experiments were carried out at room temperature.

When studying the dependence of the emission intensities at 405 and 500 nm on incident laser intensity, the pump laser intensity was attenuated in a controlled way by intercalating in the pumping beam path a quartz cell with different pressures of CS_2 [14].

In all the experiments the photolysed sample was static; thus, uncertainties in the concentrations of the photoinitiator and quenchers could result from the depletion of the initial substances and the build-up of reaction products over the course of a photolysis run. In absence of the aliphatic amine, it was checked that the absorption spectrum of each sample changed by less than 2% after irradiation by the required number of laser shots.

2.3. Materials

Acetonitrile (Scharlau, far UV HPLC grade), 2-propanol (IPA) (Normasolv, extra pure), ethanol (MERCK, absolute GR) and chloroform (MERCK, GR) were used as received. Ethyl acetate (Sigma-Aldrich, HPLC grade) was dried over molecular sieves with a pore diameter of 4 \AA .

*p*NA (Aldrich, 99) was recrystallized from water. DEELA (Scharlau, pure) was distilled under reduced pressure prior to use. Both amines were kept in the dark at low temperature and under an inert atmosphere.

1,4-Benzenediamine (BDA) (Ferosa, techn.) and trifluoroacetic anhydride (Aldrich, 99) were used as received.

Aniline (Panreac) was treated with a saturated solution of Na_2CO_3 and distilled under reduced pressure (b.p. = 184.4 $^\circ\text{C}$). Nitrobenzene (Merck for synthesis) was dried in successive steps over CaCl_2 , anhydrous MgSO_4 and CaH_2 , and then, after being filtered, was distilled under reduced pressure (b.p. = 85 $^\circ\text{C}$, 7 mmHg).

2.4. Spectroscopy of *p*-nitroaniline and analysis of its photolysed products

The UV absorption spectra of the samples were recorded at room temperature with both Perkin-Elmer Lambda 16 and

Shimadzu UV-265FS spectrophotometers. Fluorescence and phosphorescence spectra from the samples were recorded with a Perkin-Elmer LS-50B luminescence spectrometer at room temperature and at 77 K (using liquid nitrogen as coolant), respectively.

The products derived from the photolysis and photoreduction reactions of *p*NA (in absence and in presence of a tertiary amine, respectively) were analysed using a Hewlett Packard G1800A (GCD system) gas chromatographer–mass spectrometer (GC–MS). A home-made fused silica column ($L = 20$ m, i.d. = 0.25 mm, stationary phase ov-1) was used. A column temperature of 160 $^\circ\text{C}$ and Helium as carrier gas were selected.

The products to analyse, basically aliphatic and aromatic amino compounds, have high boiling points and, consequently, they cannot be detected directly with a GC–MS under the above-mentioned conditions. Therefore, and according to a method described previously [15], all the solutions to be analysed were firstly treated with trifluoroacetic anhydride in order to obtain the corresponding trifluoroacetyl derivatives which are more volatile than the initial amino compounds.

3. Results and discussion

3.1. Spectroscopic characteristics

The absorption spectrum of *p*NA in a 10^{-4} M ethyl acetate solution is shown in Fig. 2. The clear maximum observed at 356 nm corresponds to a π – π^* absorption band with some mixing n – π^* character [16]. This longest-wavelength absorption band of *p*NA is red-shifted with respect to the spectrum of nitrobenzene. This difference in the electronic absorption spectrum of both species has been discussed in terms of mesomeric and steric interactions induced by the *para* substituent [17]; an effect that is larger when the substituent group is electron-donating, as is the case of the NH_2 group of *p*NA [18]. The longest-wavelength absorption maxima of *p*NA in various solvents are tabulated in Table 1. The bathochromic shift is larger as the dielectric constant and the

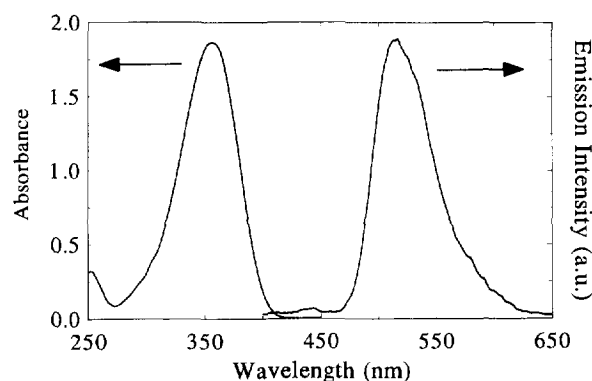


Fig. 2. Absorption and phosphorescence spectra (at 77 K) of a 10^{-4} M ethyl acetate solution of *p*-nitroaniline. Excitation wavelength: 356 nm.

Table 1

UV absorption characteristics of *p*-nitroaniline in several solvents: λ_{\max} , absorption maximum (nm); ϵ , molar absorption coefficient ($\text{mol}^{-1} \text{l cm}^{-1}$)

Solvent	λ_{\max}	$\log \epsilon_{\max}$	$\log \epsilon_{308}$	$\log \epsilon_{313}$	$\log \epsilon_{337}$	$\log \epsilon_{365}$
Chloroform	348	4.23	3.78	3.90	4.19	4.14
Ethyl acetate	356	4.22	3.61	3.72	4.12	4.19
Acetonitrile	364	4.14	3.44	3.56	3.96	4.14
Ethanol	371	4.17	3.40	3.48	3.91	4.16
2-Propanol	375	4.18	3.36	3.43	3.87	4.15

protic character of the solvent increases. The molar absorption coefficients at the wavelengths selected for the steady-state (313 and 365 nm) and laser (308 and 337 nm) photolysis studies of *p*NA are also included in Table 1. The presence of a tertiary amine in the solution does not induce significant variations in the absorption characteristics of the initiator as described above.

The phosphorescence spectrum of a 10^{-4} M ethyl acetate solution of *p*NA, registered at 77 K, is also shown in Fig. 2. The excitation wavelength was 356 nm and the delay time between excitation and detection 0.1 ms. This nitro-compound does not exhibit detectable fluorescence, which is an indication of a high intersystem crossing efficiency from the almost degenerate low-energy singlet states of *p*NA [16] so that, the excitation energy rapidly transfers to the triplet manifold that results mostly in phosphorescence emission [6]. It has been reported [6] that the ratio between the quantum yields of phosphorescence and fluorescence (Φ_p/Φ_f) in *p*NA depends on the polarity of the medium; an increase in solvent polarity induces fluorescence where there was none or produces an intensification of the fluorescence.

Phosphorescence emission centred at 510 nm was intense with a triplet lifetime of 300 ms at 77 K, which agrees well with previous results [16]. From the intercept point of the lowest wavelength of the phosphorescence emission curve with the abscise axis it could be deduced the 0–0 position of this band to be at 441 nm. This result agrees well with predictions from theoretical studies on the energy levels of this molecule [16].

Two characteristics of the phosphorescence emission allow us to confirm the $\pi\pi^*$ character of the lowest triplet state of the *p*NA: The lifetime of the triplet state at 77 K is much longer than the few milliseconds typical of $n\pi^*$ triplets, and the emission spectrum shows none of the vibrational fine structure normally associated with the phosphorescence from $n\pi^*$ states [17].

3.2. Steady-state photolysis of *p*-nitroaniline

Steady-state photolysis studies of *p*NA with irradiation at 313 nm and 365 nm were carried out on ethyl acetate solutions with initiator concentrations of 1.4×10^{-4} M and 6.3×10^{-5} M, respectively. Quantum yields of chromophore disappearance, ϕ_d were determined by UV–visible spectroscopy by following the decrease in the maximum of the ini-

ator absorption band (356 nm) with irradiation time as has been reported previously [19]. The steady-state photolysis of *p*NA is characterized by a low quantum yield, $\phi_d = 2 \times 10^{-3}$, reflecting its stability under UV irradiation.

The quantum yield of initiator disappearance does not show a significant variation over the wavelength region 313–365 nm and over the *p*NA concentration range 10^{-3} – 10^{-5} M. In addition, the parameters ϕ_d determined in nitrogen-purged and aerated solutions are, within experimental error, approximately equal. The fact that oxygen does not quench the process indicates that the reaction occurs from a very short-lived triplet state, as will be later confirmed in experiments performed under laser irradiation. This behaviour has been detected previously for other photoinitiators such as benzophenone derivatives [20].

3.2.1. Photoreduction quantum yields

Hydrogen abstraction by the lowest triplet state of *p*NA can be induced photochemically resulting in the photoreduction of this molecule [5]. In the present study, this reaction is analysed in the presence of the tertiary amine DEELA, acting as reducing agent. The DEELA compound is not volatile at room temperature (b.p. 160 °C), and does not absorb significantly at wavelengths longer than 260 nm.

The photoreduction process of *p*NA was followed by UV–visible spectroscopy. Fig. 3 shows the dependence on the irradiation time of the absorption spectrum for an ethyl acetate solution of *p*NA/DEELA in a molar proportion 1/10 irradiated at 313 nm under anaerobic conditions. The chromophore disappearance as revealed by the decrease in its absorption maximum is accompanied by an increase of the absorption intensity at shorter wavelengths. In addition, after irradiation times longer than 70 min, where the conversion of *p*NA is high ($\approx 60\%$), it does appear a new absorption band centred at ≈ 320 nm and the intensity at ≈ 253 nm becomes much more prominent. These features could be ascribed to absorption from the photoreduction products.

The quantum yields of *p*NA photoreduction by DEELA, ϕ_r , derived from the evolution of its UV absorption spectra

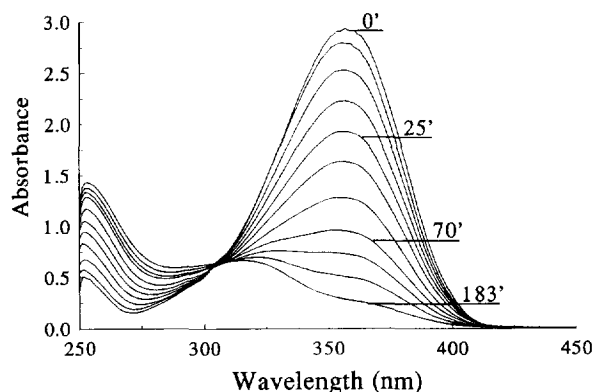


Fig. 3. Dependence of the UV–visible absorption spectrum of a 1.8×10^{-4} M ethyl acetate solution of *p*-nitroaniline with a molar proportion of 2-(*N,N*-diethylamino)ethanol 1/10 on the irradiation time under steady-state conditions in an anaerobic atmosphere. Irradiation wavelength: 313 nm.

Table 2

Photoreduction quantum yields (ϕ_r) of *p*-nitroaniline (*p*NA) in the presence of different molar proportions of 2-(*N,N*-diethylamino)ethanol (DEELA) under steady-state conditions at different irradiation wavelengths (λ_{irr}) and atmosphere conditions

<i>p</i> NA/DEELA	λ_{irr} (nm)	Atmosphere	ϕ_r
1/0	313	Anaerobic	2.0×10^{-3}
1/10	313	Anaerobic	5.3×10^{-2}
1/10	313	Aerobic	2.7×10^{-3}
1/10	365	Aaaerobic	3.5×10^{-2}
1/20	365	Anaerobic	5.3×10^{-2}
1/20	365	Aerobic	1.9×10^{-3}

under different experimental conditions, are summarized in Table 2. This parameter remains relatively unaffected when the irradiation wavelength changes from 313 to 365 nm or when the molar proportion *p*NA/DEELA changes from 1/10 to 1/20. On the other hand, the photoreduction quantum yields are critically dependent on the presence of oxygen which reduces their values by a factor up to ≈ 20 . In addition, the oxygen inhibits the new absorption band at 320 nm and induces an increase of the absorption in the 400 nm spectral region due to the generation of photooxidation products responsible for the yellow colour that *p*NA solution acquires as the reaction progresses. In the laser experiments discussed later the phosphorescence emission from *p*NA was found to be independent of the oxygen concentration in the solution. Thus, the influence of the oxygen on the photoreduction kinetics can not be ascribed to a quenching process of the lowest triplet state of *p*NA. However, the high reactivity of oxygen with the α -aminoalkyl radicals derived from the tertiary amine via a chain reaction [21] can be a pathway able to compete effectively with *p*NA photoreduction at the same time that leads to a reduction on the effective concentration of the reducing agent in the solution.

The presence of a tertiary amine as coinitiator induces an increase, of at least one order of magnitude, in the chromophore disappearance quantum yield with respect to that determined in the photolysis process. Nevertheless, the *p*NA photoreduction induced by DEELA takes place with lower efficiency than the same process induced by other families of photoinitiators, (such as benzophenone ($\phi_r \approx 1$) [22] or thioxanthenes derivatives ($\phi_r \approx 0.6$) [23]), under the same experimental conditions. This photochemical behaviour could be related to the intramolecular charge transfer character of the lowest triplet state of *p*NA, where charge transfer from its amino group to the aromatic ring is accentuated by the presence of the nitro group as an electron acceptor [4].

It is difficult to determine the precise mechanism of a photoreduction event; electron–proton transfer and hydrogen atom transfer could be considered as two elementary photoprocesses responsible for photoreduction of the nitro compounds [5]. These two processes work concurrently and it is difficult to assess their relative importance, although several factors, such as the basicity of the solution, the protonic character of the solvent, and the polarity of the medium, could be

conditioning the relative degree of participation of both mechanisms in the photoreduction process [24]. In order to characterize the photoreduction mechanism of *p*NA some experiments were carried out, where the tertiary amine was replaced by a good hydrogen donor, such as 2-propanol (IPA). The irradiation at 365 nm of an ethyl acetate solution with a molar proportion *p*NA/IPA 1/10 induces a photochemical behaviour similar to that observed in the *p*NA photolysis in absence of reducing agent. In addition, the quantum yield of *p*NA disappearance induced by the presence of alcohol, $\phi_r = 2 \times 10^{-3}$, is equal to that determined in the photolysis of pure *p*NA. Very likely, *p*NA is sterically hindered for direct hydrogen abstraction to occur, but is efficiently photoreduced by amines when the electron–proton transfer prevails [24], lending further support to the charge transfer character of the lowest triplet state of the initiator.

3.3. Laser pulsed photolysis of *p*-nitroaniline at 308 nm

3.3.1. Emission from the triplet state

The laser pulsed irradiation at 308 nm of a 2.5×10^{-3} M solution of *p*NA in ethyl acetate induces a spectral emission characterized by a structureless broad band in the range 470–600 nm (see Fig. 4). This band matches the spectral characteristics of the emission registered with the spectrometer at 77 K and 356 nm excitation wavelength (Fig. 2) and, consequently, could be assigned to phosphorescence from the first triplet state ($^3(\pi\pi^*)$) of *p*NA [6].

In Fig. 4 is also presented the dependence of the emission spectrum on *p*NA concentration after laser irradiation at 308 nm. A weak emission band centred at 360 nm appears at very low concentration of *p*NA (5×10^{-6} M). This band could be tentatively assigned to fluorescence emission from the first singlet state of the molecule [6]. Its disappearance when the concentration of *p*NA increases could be due to a reabsorption process since, as seen in Fig. 2, this molecule presents an absorption maximum at 356 nm. The spectroscopic features described above are modified neither by replacing ethyl acetate with acetonitrile as *p*NA solvent nor

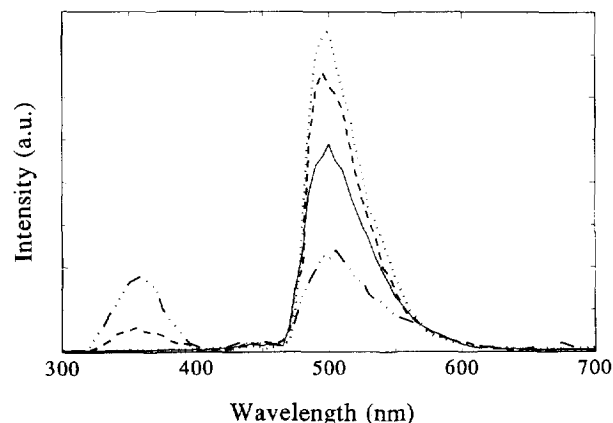


Fig. 4. Emission spectra of *p*-nitroaniline solutions in ethyl acetate after laser irradiation at 308 nm: 2.5×10^{-3} M (solid line), 5×10^{-4} M (dotted line), 5×10^{-5} M (dashed line), and 5×10^{-6} M (dotted and dashed line).

by irradiating the sample for a long time (around 3 h at 1 Hz repetition rate). No delayed fluorescence from the excited singlet state of the initiator was observed; therefore, the triplet–triplet annihilation reaction could be neglected [25].

The temporal evolution of the phosphorescence emission at room temperature reveals that the lifetime of the *p*NA triplet state is, in all solutions, less than 30 ns. The actual value for the lifetime could not be determined because it is convoluted with the time profile of the photolysis laser at 308 nm. The cause of this short lifetime cannot be ascribed to an intermolecular quenching process: if oxygen quenching of this triplet state is assumed to be diffusion controlled, $k_{\text{dif}} \approx 10^9 \text{ M}^{-1} \text{ s}^{-1}$, what implies a deactivation rate constant of $\approx 10^6 \text{ s}^{-1}$ for an oxygen concentration $[\text{O}_2] \approx 10^{-3} \text{ M}$. Thus, the triplet lifetime should be $\approx 1 \mu\text{s}$, orders of magnitude longer than the experimentally obtained value. To the best of our knowledge, there are no data reported in the literature on the lifetime of the lowest triplet state of *p*NA at room temperature. However, it is known that some aromatic nitro compounds have very short triplet lifetimes (hundred of picoseconds) due to very rapid and efficient radiationless processes [26]. The short lifetime of *p*NA triplet state makes this species insensitive to the presence of the dissolved oxygen in the medium.

The quantum yield of *p*NA disappearance in ethyl acetate solution induced by laser irradiation at 308 nm was determined by UV–visible spectroscopy and its value, $\phi_a = 4 \times 10^{-3}$, is similar to that determined under steady-state irradiation conditions.

To gain a deeper insight into the *p*NA photochemistry, some experiments were carried out to analyse the influence of the different chromophore groups present in the nitro-compound. To this end, ethyl acetate solutions of aniline and nitrobenzene were photolysed under the same experimental conditions described above. The irradiation at 308 nm of a $7 \times 10^{-3} \text{ M}$ aniline solution is followed by an intense emission centred at 335 nm that could be ascribed to fluorescence [27]. As in previous studies [28], no phosphorescence emission was detected at room temperature. Nitrobenzene in a $3 \times 10^{-3} \text{ M}$ ethyl acetate solution irradiated at 308 nm neither fluoresces nor phosphoresces, in good agreement with previous studies reported in the literature [29]. The spectroscopic characteristics observed for nitrobenzene and aniline at 308 nm irradiation are independent of the optical density of the solutions. In addition, the irradiation of a mixture 1:1 in volume of aniline and nitrobenzene solutions with concentrations $1.7 \times 10^{-3} \text{ M}$ and $1.5 \times 10^{-3} \text{ M}$, respectively (to ensure equal optical density of both chromophore groups at 308 nm), induces an emission identical to that registered for aniline alone. This result is in agreement with the description of the nitrobenzene photoreduction by amines as a low efficient process leading to aniline as final product [24]. Consequently, the photophysical characteristics of nitrobenzene are significantly modified by the presence of a NH_2 group as *para* substituent, inducing changes in its electronic struc-

ture that could be reflected in the photochemical behaviour of *p*NA.

3.3.2. Laser photoreduction of *p*-nitroaniline

The experiments were carried out adding different amounts of DEELA to a constant concentration, $3 \times 10^{-4} \text{ M}$, of *p*NA and irradiating the resulting solutions at 308 nm (XeCl laser). The following *p*NA/DEELA molar proportions were selected: 1/10, 1/20, 1/50 and 1/100. The tertiary amine used as reducing agent has negligible absorption at 308 nm; even at the highest concentration used ($3 \times 10^{-2} \text{ M}$), its molar absorption coefficient is at least 10^4 times lower than that of *p*NA.

The presence of DEELA causes the appearance of a new emission, very strong, with the maximum centred at 405 nm (see Fig. 5) and, once more, with lifetime below the experimental detection limit ($\approx 30 \text{ ns}$). At low amine concentration, both the *p*NA phosphorescence and the new emission are simultaneously seen. As the amine proportion in the solution increases, the new emission becomes more prominent until finally, at high concentrations, it is practically the only one observed.

The intensity of the 405 nm emission increases and the phosphorescence of *p*NA decreases with the number of irradiation pulses. The observed dependence becomes stronger when the molar proportion of DEELA in the sample increases. Fig. 6 represents the intensity of the 405 nm emission as a function of the number of photolysis laser pulses for solutions with *p*NA/DEELA molar proportions 1/10, 1/50 and 1/100, respectively. When the concentration of amine is low, the intensity of the emission appears to be independent of the number of irradiation pulses, within the experimental errors, while at the highest amine concentration the emission intensity increases almost exponentially. It must be pointed out that, during laser irradiation, the colourless *p*NA solution in presence of DEELA changes its colour towards a slightly different one, with a yellow component. In addition, the intensity of the emission at 405 nm was found to be critically

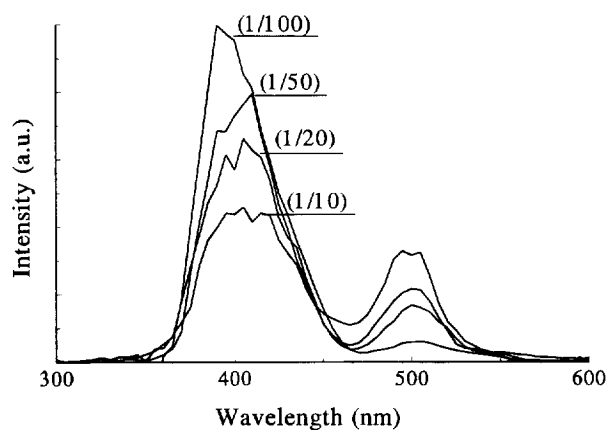


Fig. 5. Emission spectra of a $3 \times 10^{-4} \text{ M}$ ethyl acetate solution of *p*-nitroaniline (*p*NA) after laser irradiation at 308 nm with different molar proportions of 2-(*N,N*-diethylamino)ethanol (DEELA). The (*p*NA/DEELA) proportions are indicated in parenthesis.

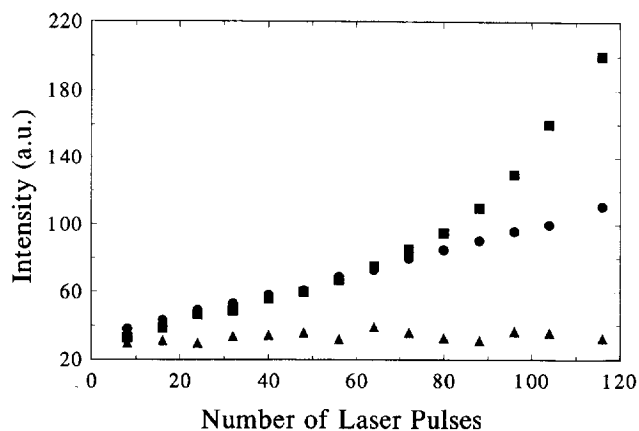


Fig. 6. Dependence of the emission intensity at 405 nm on the number of photolysis laser pulses at 308 nm for a 3×10^{-4} M ethyl acetate solution of *p*-nitroaniline with different molar proportions of 2-(*N,N*-diethylamino)-ethanol: *p*NA/DEELA = 1/10 (\blacktriangle), 1/50 (\bullet) and 1/100 (\blacksquare) respectively.

dependent on the presence of oxygen, in spite of the fact that the photoreduction occurs from a short-lived triplet state, which is probably due to the aforementioned photo-oxidation process of the tertiary amine under aerobic conditions. Consistently, a higher yield of this process was observed when carefully deoxygenated solutions placed in cells sealed off under vacuum prior to UV excitation were used.

When the aliphatic amine DEELA was replaced by a good hydrogen donor, such as IPA, the emission centred at 405 nm appears just as a shoulder on the *p*NA phosphorescence band, even when the concentrations of IPA as high as 3×10^{-2} M were added to the 3×10^{-4} M ethyl acetate solution of *p*NA. This result indicates that the photoreduction leads to the same transient or final product than that induced by amines but with a much lower quantum yield.

3.3.3. Photoreduction quantum yields

Quantum yields ϕ_r for the disappearance of *p*NA were determined by UV–visible spectroscopy, measuring the decrease of the absorption band at 356 nm. The values obtained for ϕ_r in a deoxygenated 1.3×10^{-3} M ethyl acetate solution of *p*NA/DEELA 1/50, irradiated with 308 nm pulses of different energy at 1 Hz repetition rate for time intervals up to three hours are shown in Table 3. The quantum yield decreases slightly as the irradiation time increases, due probably to absorption by photoreduction products, but does not show any significant variation over the photolysis energy range 0.5–3 mJ. No variation in the value of ϕ_r is observed either if the *p*NA concentration is decreased to 3×10^{-4} M.

Also reported in Table 3 are the values of ϕ_r for deoxygenated 3×10^{-4} M ethyl acetate solutions of *p*NA/DEELA in molar proportions 1/20 and 1/100. After two hours irradiation, the photoreduction quantum yield is slightly higher for the solutions with the highest amine concentration. The highest value of ϕ_r , 2.8×10^{-2} , is obtained for the 1/100 solution after laser irradiation during 10 min.

The evolution of the absorption spectra of *p*NA/DEELA solutions in molar proportions 1/20 and 1/100, irradiated

with 308 nm pulses at 1 Hz repetition rate under anaerobic conditions is presented in Fig. 7. It is observed a behaviour with irradiation time similar to that described under steady-state irradiation conditions (see Fig. 3). Irradiation for 2 h of the solution with a molar proportion *p*NA/DEELA 1/100 leads to a drastic change in the absorption spectrum; the absorption band of *p*NA centred at 356 nm splits into two overlapping bands with maxima at 315 nm and 375 nm, respectively, which could be ascribed to absorption by photoreduction products.

The estimated quantum yields ϕ_r under laser irradiation are of the same order of magnitude as those determined in the steady-state photolysis. The apparent inefficient photoreduction of *p*NA by the tertiary amine DEELA, as compared with the quantum yields induced by other photoinitiators, could be attributed to the presence in *p*NA molecules of faster competing radiationless deactivation processes, which result in the short lifetime detected for the lowest triplet state of *p*NA.

Table 3

Photoreduction quantum yields (ϕ_r) of *p*-nitroaniline (*p*NA) in the presence of different molar proportions of 2-(*N,N*-diethylamino)ethanol (DEELA) under pulsed laser irradiation at 308 nm and 1 Hz repetition rate: t_{irr} , irradiation time

<i>p</i> NA/DEELA ^a	t_{irr} (nm)	ϕ_r
1/0	180 ^b	4.5×10^{-3}
1/50	60 ^b	1.8×10^{-2}
1/50	120 ^b	1.2×10^{-2}
1/50	180 ^b	1.2×10^{-2}
1/50	180 ^c	1.3×10^{-2}
1/50	360 ^c	1.4×10^{-2}
1/20	120 ^b	6.8×10^{-3}
1/100	10 ^b	2.8×10^{-2}
1/100	120 ^b	9.9×10^{-3}

^a [*p*NA] = 1.3×10^{-3} M.

^b Pump energy: 3 mJ per pulse.

^c Pump energy: 0.5 mJ per pulse.

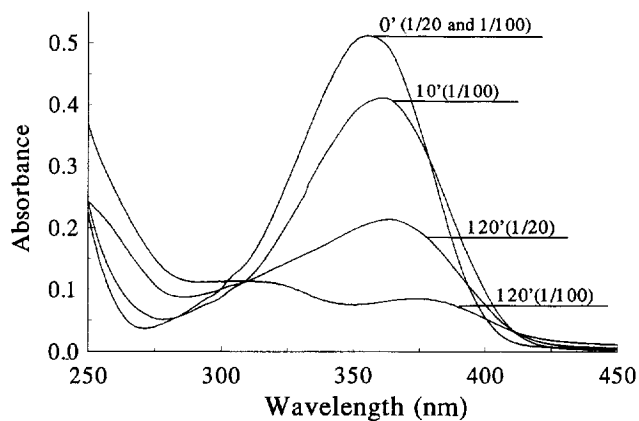


Fig. 7. UV–visible absorption spectra at different irradiation times of 3×10^{-4} M ethyl acetate solutions of *p*-nitroaniline with different molar proportions of 2-(*N,N*-diethylamino)ethanol after laser irradiation at 308 nm and 1 Hz repetition rate under anaerobic conditions. The (*p*NA/DEELA) proportions are indicated in parenthesis.

3.3.4. Laser intensity dependence of the emissions at 405 nm and 500 nm

Measurements of the dependence on irradiation laser intensity of the emissions at 405 nm and 500 nm from solutions of *p*NA in ethyl acetate with and without DEELA, respectively, were carried out. In these experiments, the concentration of *p*NA was 3×10^{-4} M, and the molar proportion of *p*NA/DEELA was chosen to be 1/10, in the region where the intensity of the 405 nm emission was independent of the irradiation time.

The probability of biphotonic absorption, W , in a sequential process in absence of saturation is quadratically dependent on the laser intensity I [30]:

$$W \propto I^2 \quad (1)$$

Thus, a sequential biphotonic absorption should yield a straight line with slope 2 in a log–log representation of the intensity of the observed emission *versus* the intensity of the incident pump intensity. In Fig. 8 it is shown such a representation for the emissions at 405 nm and 500 nm. Each point in this figure is an average over 32 laser shots. The experimentally obtained slope for the 405 nm emission is 1.8 ± 0.1 , close to the theoretically expected value for a sequential two-photon absorption. The error quoted corresponds to one standard deviation of the mean. The discrepancy with the theoretical value is of the expected magnitude in this type of measurements in which the pump beam is mildly focused [31]. Thus, it can be concluded that the emission centred at 405 nm follows a single-pulse two-photon sequential absorption.

The behaviour of the emission at 500 nm is totally different. In this case, the value found for the slope, 0.90 ± 0.04 , is close to the single-photon absorption value of 1, confirming the assignation of this emission to the *p*NA phosphorescence.

3.4. Laser pulsed photolysis of *p*-nitroaniline at 337 nm

Irradiation of a 5×10^{-4} M ethyl acetate solution of *p*NA with pulses from a N_2 laser (337 nm) induced phosphores-

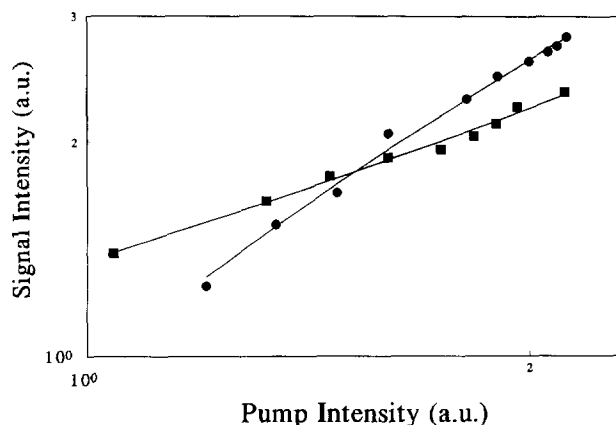


Fig. 8. Pump laser intensity dependence of the emissions at 405 nm (●) and 500 nm (■). The solid lines represent the best linear fits to the data points.

cence emission from the initiator with the same spectroscopic and temporal characteristics as those observed after the laser irradiation at 308 nm. Likewise, the irradiation at 337 nm of the above *p*NA solution incorporating different molar proportions of the tertiary amine DEELA as coinitiator induces both the new emission centred at 405 nm and the decrease of the *p*NA phosphorescence at 500 nm. The detection of the 405 nm emission after irradiation with the 10 ns N_2 -laser pulses allows us to establish 10 ns as the upper limit of the time required to generate the *p*NA photoreduction products responsible for this emission. These results, together with those obtained in the steady-state photolysis experiments, allow us to conclude that the photoreduction mechanism of *p*NA by an aliphatic tertiary amine is independent of the radiation wavelength.

3.5. Analysis of the initiator photolysis products

Further information about the *p*NA photoreduction mechanism can be obtained by studying the nature of the products generated in its photolysis. To this end, ethyl acetate solutions of *p*NA in presence of the tertiary amine were irradiated under both steady-state and laser photolysis conditions, and the products were analysed by gas chromatography–mass spectrometry. Prior to the mass analysis the irradiated samples were subjected first to solvent evaporation and then to reactions producing their trifluoroacetyl derivatives (see Section 2).

The samples analysed were solutions of *p*NA 1×10^{-3} M with molar proportions of *p*NA/DEELA 1/50 and 1/20 for laser photolysis experiments at 308 nm and steady-state photolysis studies at 365 nm, respectively. In both cases, the irradiation time was 3 h (at 1 Hz repetition rate in the pulsed laser irradiation).

In both experiments three main products were isolated after irradiation: the remanent *p*NA, the derivatized DEELA, and a compound of mass 300 with a spectrum that could be assigned to the hexafluorated derivative of BDA. This compound is the principal and final product generated in the *p*NA photoreduction induced by DEELA. The low resolution of the GC–MS as well as the treatment required to obtain the trifluoroacetyl derivatives of the photolysed samples increase the complexity of the spectra, making it impossible the unequivocal identification of other products.

The above identification of BDA as the principal *p*NA photoreduction product was confirmed by studying the behaviour under laser irradiation and the spectroscopic characteristics of pure BDA in a 6×10^{-3} M ethyl acetate solution. The laser irradiation at 308 nm of this solution induces a strong emission centred at 405 nm that completely matches both the spectrum and the lifetime of the emission band observed in the photolysis of *p*NA in presence of the tertiary

amine. This emission can be assigned to the BDA fluorescence since its spectrum is similar to that registered with the spectrometer at room temperature. In addition, the UV–visible absorption spectrum of pure BDA presents a clear maximum around 320 nm, in the same spectral region as that in the spectrum of *p*NA/DEELA 1/100 under long time irradiation.

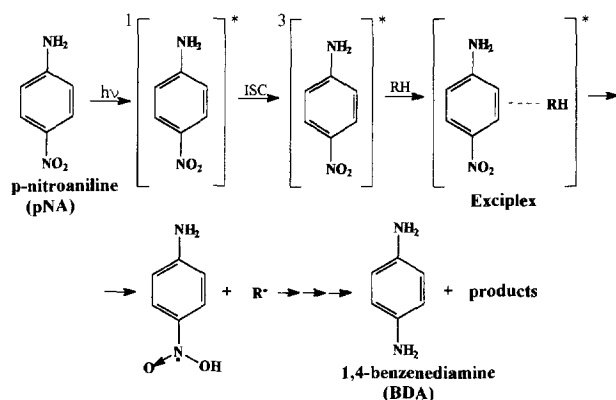
3.6. Mechanism of the *p*NA photoreduction

Taking into account all the experimental evidence presented in this paper, the reaction pathway in Scheme 1 can be tentatively proposed as the photoreduction mechanism of *p*NA by DEELA induced both under laser and steady-state photolysis.

$\text{NH}_2\text{-Ph-NO}_2\text{H}$ is postulated as the first step in the photoreduction mechanism of *p*NA, by analogy with other nitrobenzene derivatives where the hydroxyphenylaminyloxy radical $\text{Ph-NO}_2\text{H}$ has been assigned as the primary radical from hydrogen abstraction from their excited triplet states [32,33]. Taking into account the electronic spin resonance studies after photolysis of nitro compounds with hydrogen donors [34,35], it is difficult to devise a convincing pathway from $\text{NH}_2\text{-Ph-NO}_2\text{H}$ to $\text{NH}_2\text{-Ph-NH}_2$ that does not involve several intermediate dark reactions from the radical to the formation of *p*-anilin-hydroxylamine and *p*-nitrosoaniline. While it is reasonable to postulate that these intermediates should play a role in the *p*NA photoreduction mechanism, it must be recognized that direct evidence by either gas chromatography–mass spectrometry or absorption spectroscopy is still lacking.

The laser-flash photolysis studies of *p*NA described in this work allow to establish 10 ns as the upper limit of the time required to complete the photoreduction process. The present results, therefore, suggest that, in *p*NA, the rate of the intermolecular hydrogen abstraction is comparable with, or less than, other radiationless processes. In fact, rate constants for quenching by the charge-transfer mechanism are expected to be higher than those for radical-like hydrogen atom abstraction [36].

Although it is difficult to postulate a complete mechanism, the photoreduction of *p*NA to BDA should be expected to



involve several hydrogen abstractions from the tertiary amine molecules acting as coinitiators. This fact would determine the generation of several amino-radicals for each *p*NA molecule photoreduced. Consequently, and in spite of the low photoreduction activity presented by the *p*NA/DEELA solutions, the high concentration of amino-radicals could result in an enhanced efficiency on the initiation of polymerization photoinduced by this system. Studies to elucidate the molar proportion of the photoinitiator molecule photoreduced with respect to the amino-radicals generated, as well as the activity of the *p*NA/DEELA system as photoinitiator of polymerization are in progress.

Acknowledgements

J. Dabrio thanks Ministerio de Educación y Ciencia for a scholarship. This work was supported by Comisión de Investigación Científica y Técnica Project MAT94-0757.

References

- [1] R. Sastre, M. Conde, J.L. Mateo, J. Photochem. Photobiol., A: Chem 44 (1988) 111.
- [2] F. Diaz, L.H. Tagle, F. Garcia, R. Sastre, M. Conde, J.L. Mateo, F. Catalina, J. Polym. Sci. A 28 (1990) 3499.
- [3] R. Sastre, J. Dabrio, F. Diaz, F. Amat-Guerri, Communication at Symposium Iberoamericano de Polímeros, Vigo, 1992.
- [4] J. Wolleben, A.C. Testa, J. Phys. Chem. 81 (1977) 429.
- [5] D. Döpp, Top. Curr. Chem. 55 (1975) 49.
- [6] O.S. Khalil, C.J. Seliskar, S.P. McGlynn, J. Chem. Phys. 58 (1973) 1607.
- [7] R. Hurley, A.C. Testa, J. Am. Chem. Soc. 90 (1968) 1949.
- [8] L.J. Johnston, D.J. Loughnot, V. Wintgens, J.C. Scaiano, J. Am. Chem. Soc. 110 (1988) 518.
- [9] R.W. Redmond, J.C. Scaiano, L.J. Johnston, J. Am. Chem. Soc. 114 (1992) 9768.
- [10] F. Catalina, J.M. Tercero, C. Peinado, R. Sastre, J.L. Mateo, N.S. Allen, J. Photochem. Photobiol. A: Chem 50 (1989) 249.
- [11] H.G. Heller, J.R. Langan, J. Chem. Soc. Perkin Trans. 2 (1981) 341.
- [12] J.M. Figuera, R. Sastre, A. Costela, I. Garcia-Moreno, M.T. Al-Hakakk, J. Dabrio, Laser Chem. 15 (1994) 33.
- [13] M. Rodriguez, A. Costela, I. Garcia-Moreno, F. Florido, J.M. Figuera, R. Sastre, Meas. Sci. Technol. 6 (1995) 971.
- [14] H. Okabe, Photochemistry of Small Molecules, Wiley, New York, 1978, p. 218.
- [15] D.R. Knapp, Handbook of Analytical Derivatization Reactions, Wiley, New York, 1979, p. 73.
- [16] V.G. Plotnikov, V.M. Komarov, Spectrosc. Lett. 9 (1976) 265.
- [17] C.N.R. Rao, The Chemistry of the Nitro and Nitroso Groups, H. Feuer, New York, 1969.
- [18] J. Grimshaw, A.P. de Silva, Chem. Soc. Rev. 10 (1981) 181.
- [19] J.L. Mateo, J.A. Manzarbeitia, R. Sastre, J. Photochem. Photobiol. A: Chem. 40 (1987) 169.
- [20] A. Costela, J. Dabrio, J.M. Figuera, I. Garcia-Moreno, H. Gsponer, R. Sastre, J. Photochem. Photobiol. A: Chem. 99 (1995) 213.
- [21] R.S. Davidson, Radiation Curing in Polymer Science and Technology, vol. III of J.P. Fouassier, J.F. Rabek (eds.), Polymerization Mechanisms, Elsevier Applied Science, Barking, 1993, pp. 153–176.
- [22] N.S. Allen, S.J. Hardy, A.F. Jacobine, D.M. Glaser, B. Yang, D. Wolf, F. Catalina, S. Navaratnam, B.J. Parsons, J. Appl. Polym. Sci. 42 (1991) 1169.

- [23] F. Catalina, J.M. Tercero, C. Peinado, R. Sastre, J.L. Mateo, J. Photochem. Photobiol., A: Chem. 50 (1989) 249.
- [24] J. Malkin, Photophysical and Photochemical Properties of Aromatic Compounds, CRC Press, Boca Raton, FL, 1992, Chapter 14.
- [25] N.J. Turro, Modern Molecular Photochemistry, Benjamin/Cummings, CA, 1978, p. 146.
- [26] R.W. Yip, D.K. Sharma, R. Giasson, D. Gravel, J. Phys. Chem. 88 (1984) 5770.
- [27] G. Perichet, R. Chapelou, B. Pouyet, J. Photochem. 13 (1980) 67.
- [28] Ya.N. Malkin, V.A. Kuzmin, Russ. Chem. Rev. 541 (1985) 1761.
- [29] J.S. Brinen, B. Singh, J. Am. Chem. Soc. 93 (1971) 6623.
- [30] M. Martín Muñoz, Lasers, C.S.I.C. Press, Madrid, 1986, p. 202.
- [31] S. Sepiser, J. Jortner, Chem. Phys. Lett. 68 (1976) 3999.
- [32] J.A. Barltrop, N.J. Bunce, J. Am. Chem. Soc. (C) (1968) 1467.
- [33] R. Hurley, A.C. Testa, J. Am. Chem. Soc. 88 (1966) 4330.
- [34] S.K. Wong, J.K.S. Wan, Can. J. Chem. 51 (1973) 753.
- [35] G.G. Wubbels, J.W. Jordan, N.S. Mulls, J. Am. Chem. Soc. 95 (1973) 1281.
- [36] J.L. Mateo, P. Bosch, Polym. Adv. Technol. 5 (1994) 561.